



Improved Antitumor Efficacy of Hyaluronic Acid-Complexed Paclitaxel Nanoemulsions in Treating Non-Small Cell Lung Cancer

Joo-Eun Kim and Young-Joon Park*

College of Pharmacy, Ajou University, Suwon 16499, Republic of Korea

Abstract

Paclitaxel (PTX) is a effectively chemotherapeutic agent which is extensively able to treat the non-small cell lung, pancreatic, breast and other cancers. But it is a practically insoluble drug with water solubility less than 1 $\mu\text{g/mL}$, which restricts its therapeutic application. To overcome the problem, hyaluronic acid-complexed paclitaxel nanoemulsions (HPNs) were prepared by ionic complexation of paclitaxel (PTX) nanoemulsions and hyaluronic acid (HA) to specifically target non-small cell lung cancer. HPNs were composed of DL- α -tocopheryl acetate, soybean oil, polysorbate 80, ferric chloride, and HA and fabricated by high-pressure homogenization. The HPNs were 85.2 ± 7.55 nm in diameter and had a zeta potential of -35.7 ± 0.25 mV. The encapsulation efficiency was almost 100%, and the PTX content was 3.0 mg/mL. We assessed the *in vivo* antitumor efficacy of the HPNs by measuring changes in tumor volume and body weight in nude mice transplanted with CD44-overexpressing NCI-H460 xenografts and treated with a bolus dose of saline, Taxol[®], PTX nanoemulsions (PNs), or HPNs at a dose of 25 mg/kg. Suppression of cancer cell growth was higher in the PN- and HPN-treated groups than in the Taxol[®] group. In particular, HPN treatment dramatically inhibited tumor growth, likely because of the specific tumor-targeting affinity of HA for CD44-overexpressed cancer cells. The loss of body weight and organ weight did not vary significantly between the groups. It is suggest that HPNs should be used to effective nanocarrier system for targeting delivery of non-small cell lung cancer overexpressing CD44 and high solubilization of poorly soluble drug.

Key Words: Hyaluronic acid-complexed paclitaxel nanoemulsions, Specific targeting, Antitumor efficacy, Non-Small cell lung cancer

INTRODUCTION

The anticancer drug paclitaxel (PTX), derived from the bark of the Pacific yew, is a popular chemotherapeutic agent extensively used to treat non-small cell lung, ovarian, pancreatic, breast, and other cancers (Journo-Gershfeld *et al.*, 2012). PTX acts by interfering with the normal breakdown of microtubules during cell division. The drug can induce cell apoptosis (Othman *et al.*, 2001) and mitotic arrest and inhibit necessary cellular functions such as motility, transport, and mitosis (Orr *et al.*, 2003; Xin *et al.*, 2010; Baek *et al.*, 2012). However, the water solubility of PTX is less than 1 $\mu\text{g/mL}$, restricting its therapeutic application. To overcome this limitation, various formulations have been tested in clinical trials. Among them, one popular preparation is Taxol[®] (Bristol-Myers Squibb, NY, USA), a commercial product containing Cremophor EL[®] (polyoxyethylated castor oil, BASF, Ludwigshafen, German) and ethanol. Cremophor EL[®] solubilizes PTX, but can lead to serious side effects, including neurotoxicity, acute hyper-

sensitive syndrome, labored breathing, nephrotoxicity, and cardiotoxicity (Liebmann *et al.*, 1993). The compound is usually a requirement for premedication with anti-histamines and corticosteroids to decrease the risk of several hypersensitive symptoms in patients treated with Taxol[®] (Singla *et al.*, 2002).

Because of these problems, an alternate PTX formulation with excellent solubility is needed, which would target delivery of PTX to tumor cells while exerting minimal side effects. Drug-delivery systems such as albumin nanoparticles, liposomes, poly (lactic-co-glycolic acid) (PLGA) nanoparticles, lipid carriers, and polymeric micelles have been investigated to enhance the targeted delivery of PTX (Singla *et al.*, 2002; Zhao *et al.*, 2012; Yang *et al.*, 2013; Kirtane *et al.*, 2014; Park *et al.*, 2014; Sim *et al.*, 2016); however, most of these formulations have not been applied clinically because they are fabricated as new materials, not approved by the U.S. Food and Drug Administration (FDA), having a low tumor-targeting capability. Poor tumor-cell targeting can often induce serious side effects. Therefore, an active tumor-targeting delivery sys-

Open Access <https://doi.org/10.4062/biomolther.2016.261>

This is an Open Access article distributed under the terms of the Creative Commons Attribution Non-Commercial License (<http://creativecommons.org/licenses/by-nc/4.0/>) which permits unrestricted non-commercial use, distribution, and reproduction in any medium, provided the original work is properly cited.

Received Nov 24, 2016 Revised Dec 27, 2016 Accepted Dec 30, 2016
Published Online Feb 17, 2017

*Corresponding Author

E-mail: parkyj64@gmail.com
Tel: +82-31-219-3493, Fax: +82-31-219-3432

tem for PTX-based chemotherapeutics is urgently required to minimize adverse effects (Kim and Park, 2016).

Some targeting molecules such as hyaluronic acid (HA), folic acid, L-biotin, lipoproteins, and cholesterol have been investigated for active delivery of PTX to tumor tissues (Danhier *et al.*, 2009; Zhan *et al.*, 2010; Zhao *et al.*, 2010; Battistini *et al.*, 2014). Among them, HA is preferentially studied because it is composed of a negatively charged polysaccharide with repeating glucuronic acid (GlcUA) and N-acetyl-D-glucosamine (GlcNAc) units. HA specifically binds to cluster of differentiation 44 (CD44), which is a cell surface biomarker overexpressed in tumors. The specific affinity of HA to CD44 in cancer therapy provides a strategy for active tumor targeting (Matsubara *et al.*, 2000), and while many studies have leveraged this affinity, not many have applied it to active targeting in non-small cell lung cancer therapy.

In our previous study, we developed a nanoemulsion PTX carrier with a high solubilizing capacity for the poorly soluble drug (Kim and Park, 2016). In the current study, we investigated the physicochemical properties of HA-complexed PTX nanoemulsions (HPNs) as a drug carrier system, and evaluated the antitumor efficacy of PTX nanoemulsions (PNs) and HPNs in a CD44-overexpressing human non-small cell lung carcinoma cell line, NCI-H460. *In vivo* antitumor efficacy, body weight loss, and tumor tissue weight were assessed in a transplanted nude mouse model of non-small cell lung cancer.

MATERIALS AND METHODS

Materials

HA was purchased from Bioiberica (Barcelona, Spain). PTX was provided by Cipla (Mumbai, India). Soybean oil was purchased from Croda Health Care (Snaith, UK), and injectable polysorbate 80 was purchased from SEPPIC (Puteaux, France). DL- α -Tocopheryl acetate was purchased from DSM Sinochem Pharmaceuticals (Shanghai, China). D-mannitol, ferric chloride (FeCl₃), chloromethylbenzoyl chloride, and tetra-n-butyl ammonium hydroxide (TBA) were purchased from Sigma-Aldrich (St. Louis, MO, USA).

To perform *in vivo* efficacy studies, NCI-H460 (CD44⁺) human non-small cell lung cancer cells were obtained from the American Type Culture Collection (ATCC, Manassas, VA, USA). Cell culture media (RPMI 1640 and Waymouth's), penicillin, streptomycin, N-2-hydroxyethylpiperazine-N-2-ethanesulfonic acid (HEPES) buffer solution, and heat-inactivated fetal bovine serum (FBS) were purchased from Gibco Life Technologies, Inc. (Waltham, MA, USA). All other chemicals and reagents were of analytical grade.

Preparation of HPNs

HPNs were fabricated according to a previously reported method (Kim and Park, 2016). In brief, PNs were comprised of an oil phase (DL- α -tocopheryl acetate and soybean oil), surfactant (polysorbate 80), and water phase. HA (molecular weight [MW] 500 kDa) was used as a targeting molecule and the HPNs were prepared using a high-pressure homogenization method with a microfluidizer (Danhier *et al.*, 2009; Zhan *et al.*, 2010; Zhao *et al.*, 2010; Battistini *et al.*, 2014). The HA was complexed onto the surface of the PNs using chelating covalent bonding attraction (Mercê *et al.*, 2002). First, 252 mg of HA were dissolved in 84 mL of water for injection as the water

phase. Next, 300 mg of PTX and 2 mg of ferric chloride were dissolved in 20 mL of ethanol. Eight grams of polysorbate 80 were then dissolved in 7.2 g of DL- α -tocopheryl acetate and 0.8 g of soybean oil at 25°C. Next, 20 mL of ethanol containing PTX and ferric chloride was dissolved in a mixture of oil and surfactant. Thereafter, the ethanol was completely evaporated using a vacuum rotary evaporator in the oil phase mixture. The water phase with HA was then added to the previously prepared oil phase with gentle magnetic stirring for 1 h. The two-phase mixture was slowly added to a microfluidizer chamber, and the crude emulsion was further homogenized using a high-pressure homogenizer (Model M-110S, Microfluidics, Newton, MA, USA) at 15,000 psi seven times and then cooled to 20°C.

Finally, the prepared nanoemulsions were added to 500 mg D-mannitol as a cryo-protectant and were then lyophilized using a freeze dryer (Model Genesis 25XL, VirTis freeze dryer™, Warminster, PA, USA). PNs were prepared in a similar manner, without the addition of HA.

Characterization of HPNs

Particle characterization: The particle characteristics (zeta potential, polydispersity, and size of the PNs and HPNs) were evaluated by dynamic light scattering (DLS) at 25°C using a Malvern Zetasizer NanoZS™ laser scattering particle analyzer (Malvern Instruments Ltd., Malvern, UK) as reported previously (Yang *et al.*, 2013). Reconstituted PN and HPN solutions were diluted 10-fold by double-distilled water, and promptly measured at least in triplicate at 25°C.

Morphology: A lyophilized HPN sample was reconstituted with double-distilled water before measurement. HPN morphology was observed using a cryo-transmission electron microscope (cryo-TEM, FEI Tecnai G2F20, Eindhoven, The Netherlands) as reported previously (Kim and Park, 2016). Approximately 5-10 μ L of reconstituted HPN solution were deposited on the copper grid and covered by a porous carbon thin film.

The HPN droplet was blotted with a filter paper to form a thin liquid film not more than 300 nm. The droplet was then rapidly frozen in liquid ethane below -184°C. The resultant thin films of HPN solution bridged on the copper grid were immediately measured by cryo-TEM.

HPN drug content

High-performance liquid chromatography (HPLC) analysis: PTX in the inner core of PNs and HPNs was measured using HPLC with a separation module and a 227-nm fluorescent detector (Agilent 1200 series, Santa Clara, CA, USA) as reported previously (Zhao *et al.*, 2012; Yang *et al.*, 2013). A pentafluorophenyl silica column (Phenomenex, 250 mm \times 4.6 mm; 5 μ m, Torrance, CA, USA) was used for analysis, with a column temperature of 30 \pm 5°C. The mobile phase consisted of water and acetonitrile (11:9 v/v). The solution was then filtered through a 0.45- μ m membrane and degassed using an online degasser. The diluent solution was prepared by mixing 1,000 mL of methanol with 200 μ L of glacial acetic acid. The injection volume was 20 μ L and the flow rate was approximately 1.2 mL/min. Exactly 30 mg of PTX was dissolved in diluent solutions to a concentration of 1-30 μ g/mL. The calibration graph was rectilinear with a correlation coefficient of 0.999. The standard deviation of accuracy and precision was <3%.

Drug content (DC) and encapsulation efficiency (EE):

Table 1. Physicochemical characterization of PNs and HPNs

Test substances	Mean diameter (nm)	Polydispersity index (PDI)	Zeta potential (mV)	Encapsulation efficiency (%) ^a	Drug content (mg/mL) ^b
PNs	71.7 ± 8.81	0.20 ± 0.04	28.6 ± 0.88	100.2 ± 0.35	3.00 ± 0.01
HPNs	85.2 ± 7.55	0.21 ± 0.05	-35.7 ± 0.25	100.4 ± 0.22	3.00 ± 0.01

Data are presented as mean ± SD (n=3).

^aEncapsulation efficiency (%)=(amount of PTX encapsulated in PNs or HPNs/amount of the feeding PTX)×100%.

^bDrug content (mg/mL)=(amount of PTX in PNs or HPNs/amount of the feeding material and PTX in the 10-mL vial).

PNs, paclitaxel nanoemulsions; HPNs, hyaluronic acid-complexed paclitaxel nanoemulsions.

The amount of PTX entrapped in PNs or HPNs was calculated as follows:

DC (mg/mL) was calculated by dividing the amount of entrapped PTX in the PNs or HPNs by the amount of the feeding material and PTX in the vial. EE (%) was calculated by dividing the amount of PTX encapsulated in the PNs or HPNs by the amount of PTX dose and multiplying by 100%. To evaluate the DC, 10 mL of the reconstituted PNs and HPNs were filtered through a 0.22- μ m membrane (Acro Disk 50 Vent Devices with Emflon Membrane[®] II, Pall Corp., Port Washington, NY, USA) to remove any non-entrapped PTX which could disperse in the water phase. The 1mL of filtered sample PTX encapsulated in the PNs or HPNs was diluted 100-fold by diluent solutions and was measured using the HPLC analytical method.

To evaluate the EE (Liu *et al.*, 2011b), 2 mL of the reconstituted PNs and HPNs were filtered through a 0.22- μ m membrane (Acro Disk 50 Vent Devices with Emflon Membrane[®] II) to remove any non-entrapped PTX which could disperse in the water phase. The filtered sample was centrifuged at 60,000×g for 1 h by ultracentrifuge tube (16×60 mm) with a Beckman Coulter Ultracentrifuge (Beckman Coulter, Fullerton, CA, USA) to obtain the PTX entrapped in PNs and HPNs. The centrifuged precipitant was dissolved in 1 mL of acetonitrile. The PTX encapsulated in the PNs or HPNs was measured using the HPLC analytical method described in Section 2.4.1 (Zhao *et al.*, 2012; Yang *et al.*, 2013; Kim and Park, 2016).

Antitumor efficacy

The *in vivo* antitumor efficacy of the PNs and HPNs was assessed using nude mice treated with a bolus injection of 25 mg/kg in a CD44-overexpressing NCI-H460 xenograft tumor for 6 weeks (Liu *et al.*, 2015; Xiong *et al.*, 2016).

The NCI-H460 cell line was cultured under a 5% CO₂ atmosphere at 37°C in RPMI 1640 medium containing 10% (v/v) FBS, 100 U/mL of penicillin, and 0.1 mg/mL of streptomycin. To transplant into nude mice, a minimum of 7×10⁸ NCI-H460 cells were required.

RPMI 1640 medium consisted of 1.5 g/L of sodium bicarbonate, 100 U/mL of penicillin, 0.1 mM of non-essential amino acids, 1 mM of sodium pyruvate, and 0.1 mg/mL of streptomycin, and was filtered and stored at 4°C. The medium was warmed to 37°C before use.

The NCI-H460 cells were treated with a trypsin/ethylenediaminetetraacetic acid (EDTA) solution and isolated from the 225-cm² culture flask; 1×10⁷ cells were suspended in 0.3 mL of RPMI 1640. To transplant the tumor cells into the nude mice, 0.3 mL of the respective cell suspensions was subcutaneously administered into the flank of each mouse using a 1-mL 23-gauge syringe.

Within 7 days of administration, a tumor could be seen in the left or right flank. When tumor sizes reached at least 200 mm³, the cancer-transplanted nude mice were divided into four groups (n=6 per group) of similar average tumor sizes. Group 1 received physiological saline (control); group 2 was treated with Taxol[®] (positive control, 25 mg/kg); group 3 was treated with PNs (25 mg/kg); group 4 was treated with HPNs (25 mg/kg). In the control group, only hypertonic saline was administered to monitor untreated cancer cell growth (Liu *et al.*, 2015). The formulations were administered 3 times via the caudal vein by the interval of 4 day for 8 days. The total observation period was observed for 6 weeks.

To evaluate the antitumor activity of each treatment, changes in tumor size were determined in the treated mice 2-3 times per week at intervals of approximately 4 days from the time point at which cancer cell growth was first identified. Tumors were measured with vernier calipers, and tumor size was calculated from the length and width according to the following formula (Liu *et al.*, 2011a; Yang *et al.*, 2013; Xiong *et al.*, 2016):

Tumor size (mm³)=length (mm)×[width (mm)]²/2, where width was the shortest diameter and length the longest diameter.

Change in body weight and tissue weight

Changes in body weight of the mice treated with saline, Taxol[®], PNs, or HPNs with a bolus injection of 25 mg/kg in tumor-transplanted CD44-overexpressing NCI-H460 xenografts was measured using a precision electronic balance 1-2 times per week at intervals of approximately 4 day for 6 weeks (Yang *et al.*, 2013).

The experiment was terminated after approximately 6 weeks at the discretion of the investigator. The mice were sacrificed and the tumor, liver, heart, lungs, spleen, and kidneys (right and left) were collected and weighed using a precision electronic balance (Yang *et al.*, 2013). All experiments were performed at least five times; data are expressed as the means ± standard deviation (SD). Statistical comparisons between each groups were performed using Student's t test. *p*< 0.05 was considered significant.

RESULTS

HPN characterization

As shown in Table 1, the PN and HPN zeta potential was 28.6 ± 0.88 and -35.7 ± 0.25 mV, respectively. Although the PNs had a positive zeta potential value of approximately 29 mV, the HPNs were negatively charged because their surface was coated with HA. The PNs and HPNs had opposite zeta

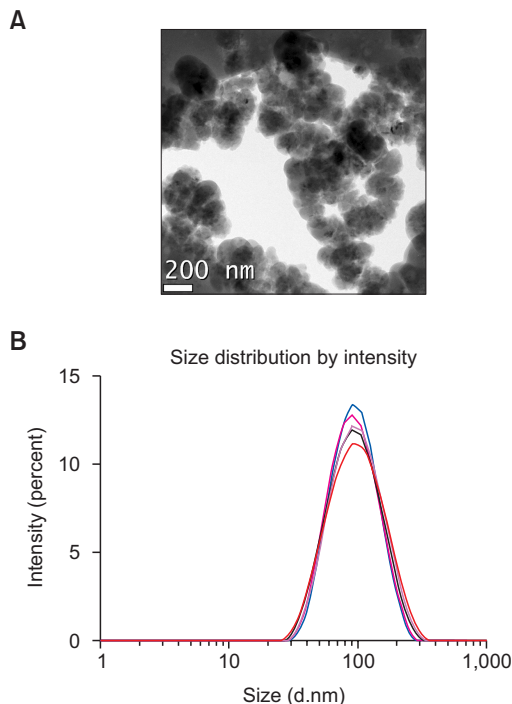


Fig. 1. Cryogenic transmission electron microscopy (cryo-TEM, A) and size distribution (B) of hyaluronic acid-complexed paclitaxel nanoemulsions. Scale bar in the cryo-TEM image: 200 nm.

potential values of approximately -36 mV.

Particle characteristics (polydispersity and size) were measured by DLS. The mean diameter of the PNs and HPNs was 71.7 ± 8.81 and 85.2 ± 7.55 nm, respectively. The polydispersity index of the PNs and HPNs was 0.20 ± 0.04 and 0.21 ± 0.05 , respectively, with a narrow size distribution.

HPN morphology imaged with cryo-TEM is shown in Fig. 1A. The nanoparticles appear to be attached; their size appeared to be 100-200 nm. As shown in Fig. 1B, although DLS determined a z-average diameter of 83.67 nm in the HPNs, the actual particle size was slightly larger.

HPN mean particle size was greater than PN particle size ($p < 0.05$) due to the presence of HA on the surface of the HPNs. The HPN particle size was greater than approximately 10-15 nm when compared to the PN particle size.

It is known that particle size alters the pharmacokinetics by affecting tissue distribution and excretion; nanocarriers with a small particle size (< 200 nm) display increased drug accumulation in tumor cells because of the enhanced permeability and retention (EPR) effect (Davis *et al.*, 2008). Given that in our study, the size of the PN and HPN was < 100 nm, drug accumulation in tumor cells was expected to be relatively high (Fang *et al.*, 2011). And high molecular weight (HMW) HA has higher affinity to CD44 than low molecular weight (LMW) HA, however, it shows lower stability during blood circulation compared to low molecular weight HA. In the previous research, we have carried out an experiment to measure the amount of HA coated on the surface of nanoemulsions using assay for chondroitin sulfate. We have confirmed that the amount of surface coating using LMW HA is more efficient and higher than that of HMW HA. So we were used LMW HA.

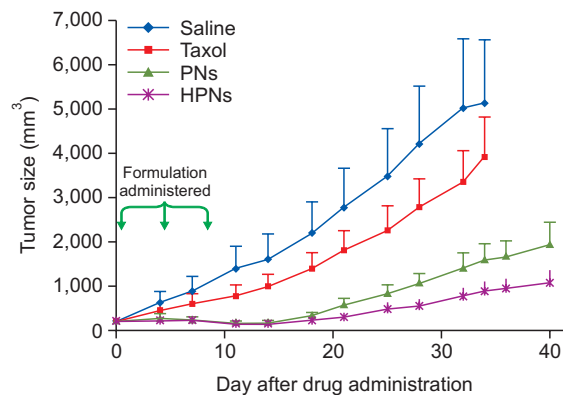


Fig. 2. Representative images of *in vivo* antitumor efficacy of saline, Taxol®, PNs, or HPNs in nude mice treated with a bolus injection of 25 mg/kg in tumor-transplanted CD44-overexpressing NCI-H460 xenografts. Variations in tumor volume are presented. Note: HPNs was $p < 0.01$ versus Saline, HPNs was $p < 0.05$ versus Taxol®, PNs, paclitaxel nanoemulsions; HPNs, hyaluronic acid-complexed paclitaxel nanoemulsions.

Finally, the particle size, morphology, and zeta potential varied greatly between the PNs and HPNs. Particle size, surface charge, and polydispersity index were all greater in the HPNs than in PNs.

Drug content (DC) of HPN

As a shown in Table 1, the EE and DC of the PNs ($n=3$) were $100.2 \pm 0.35\%$ and 3.00 ± 0.01 mg/mL, respectively. Those of the HPNs were $100.4 \pm 0.22\%$ and 3.00 ± 0.01 mg/mL, respectively. These data displayed satisfactory reproducibility. The EE was $>9.5\%$, independent of the PTX content (3.0 mg/mL) for all PN and HPN batches tested. This suggests that PTX was perfectly encapsulated in the oil phase of the nanoemulsions (Zhao *et al.*, 2008).

During preliminary studies, we determined that the PN and HPNs DC was >6 mg/mL; however, to maintain stability over time, we used <3.5 mg/mL of PTX in this study.

Antitumor efficacy

We assessed the *in vivo* antitumor efficacy of the treatment preparations by measuring the change in tumor volume and body weight of nude mice treated with a bolus dose (25 mg/kg) of saline, Taxol®, PNs, or HPNs (Zhao *et al.*, 2012; Yang *et al.*, 2013; Park *et al.*, 2014; Liu *et al.*, 2015). When tumor size did not increase, we judged the treatment to exert a strong antitumor effect; this was seen in the HPN-treated group ($p < 0.01$ versus Saline) (Fig. 2). Suppression of cancer cell growth was higher in the PN and HPN groups than in the Taxol® group ($p < 0.05$).

Inhibition of cancer cell growth in mice treated with the PNs was more efficient than in mice treated with Taxol® ($p < 0.05$). The non-small cell cancer suppression ability of the PNs was higher than that of Taxol® ($p < 0.05$), likely indicating that the PNs only passively targeted tumor cells via the EPR effect.

The HPNs reduced cancer cell growth more efficiently than the PNs administered over the study period, likely due to the presence of HA on the surface of the nanoemulsions (Kim and Park, 2016). This may also indicate that HPNs targeted tumor cells not only passively through the EPR effect, but also

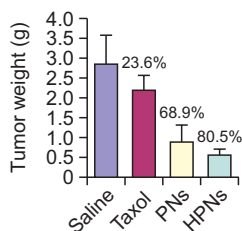


Fig. 3. Variations in tumor tissue weight at 6 weeks after an intravenous bolus injection of 25 mg/kg of saline, Taxol®, PNs, or HPNs via the caudal vein. Data are presented as means \pm SD (n=5). Note: HPNs was $p < 0.01$ versus Saline, HPNs was $p < 0.05$ versus Taxol®. PNs, paclitaxel nanoemulsions; HPN, hyaluronic acid-complexed paclitaxel nanoemulsions.

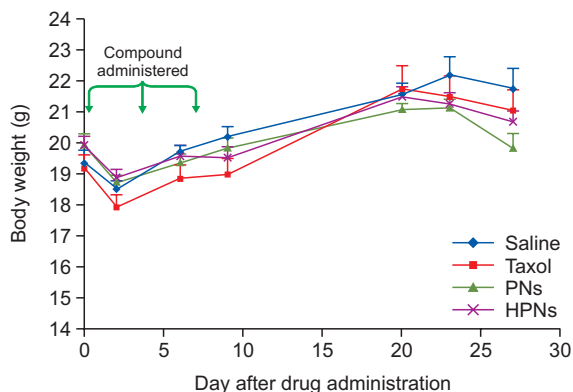


Fig. 4. Representative images of changes in body weight in mice treated with saline, Taxol®, PNs, or HPNs with a bolus injection of 25 mg/kg in tumor-transplanted CD44-overexpressing NCI-H460 xenografts. Variations in body weight are presented. PNs, paclitaxel nanoemulsions; HPN, hyaluronic acid-complexed paclitaxel nanoemulsions.

actively via binding affinity to CD44 in the xenograft (Xiong *et al.*, 2016).

Changes in tumor tissue weights at 6 weeks after treatment are shown in Fig. 3. There was significant difference in tumor weight among the groups treated saline, Taxol®, PNs, and HPNs after 6 weeks. Tumor weight was dramatically reduced by 68.9% in the PN group than in the control saline group ($p < 0.05$). Furthermore, tumor weight in mice treated with HPNs was significantly lower than in the mice from all other treatment groups, and was reduced by 80.5% compared to controls ($p < 0.01$). Tumor weight was only reduced by 23.6% in the Taxol®-treated group ($p < 0.05$).

Change in body weight and tissue weight

As shown in Fig. 4, body weight loss in mice treated with Taxol® was greater than in mice treated with saline. This implies that Taxol® exerts toxicity and adverse effects. However, mice treated with PNs or HPNs displayed a less than 10% change in body weight ($p < 0.05$); this may indicate that PNs and HPNs exert low toxicity and cause few side effects (Liu *et al.*, 2015). But, totally, there was no significant difference in body weights loss among the groups ($p > 0.05$). Changes in various organ weights 43 days after treatment are shown in Fig. 5. There was no significant difference in liver, heart, lung,

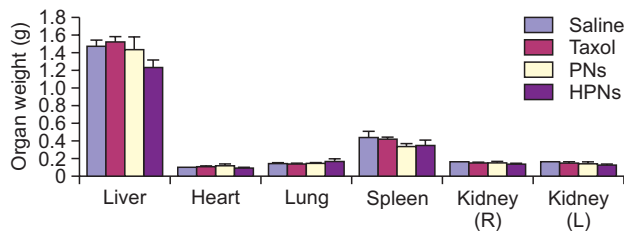


Fig. 5. Variations in organ weight in tumor-transplanted CD44-overexpressing NCI-H460 xenograft mice at 6 weeks after an intravenous bolus injection of 25 mg/kg of saline, Taxol®, PNs, or HPNs via the caudal vein. Data are presented as means \pm SD (n=5). Note: $p > 0.05$ all of them. PNs, paclitaxel nanoemulsions; HPNs, hyaluronic acid-complexed paclitaxel nanoemulsions.

spleen, and kidney weights between the groups ($p > 0.05$). Liver weights in the mice treated with HPNs were slightly reduced, but the difference was not significant ($p > 0.05$).

DISCUSSION

In this study, HPNs and PNs without HA were successfully prepared for the delivery of the poorly soluble PTX to non-small cell lung carcinomas via active tumor targeting.

HPNs were prepared using high-pressure homogenization with a microfluidizer. The PTX content was 3.0 mg/mL, and the EE was close to 100%. It was possible to fabricate a nanoemulsion with a high PTX-loading rate by dissolving PTX in the oil phase, which demonstrated a high emulsion-solubilizing capacity. Previous studies indicated that the PN and HPN DC could be higher than 6 mg/mL. To obtain an EE $> 100\%$, the incorporated PTX was located in the oil phase of the nanoemulsions (Kim and Park, 2016). However, to maintain a stable infusion formulation for an extended period, even after dilution with saline or a dextrose solution, we used 3 mg/mL of PNs and HPNs.

The particle size and zeta potential of the PNs varied greatly from those of the HPNs. The HPNs were negatively charged due to their HA surface coating. The mean particle size of the HPNs was slightly larger (10-15 nm) than that of the PNs, likely due to the presence of HA. This suggests that the HPN cores contained the nanoparticles and that the HA coating, in the μ -oxoform covalently bound to ferric chloride in the oil phase (Mercê *et al.*, 2002), played an important role in the active targeting of cancer (Mizrahy *et al.*, 2011).

We assessed *in vivo* antitumor efficacy by measuring the changes in tumor volume and body weight of the mice. Suppression of cancer cell growth was higher in the PN and HPN groups than in the Taxol® group. The non-small cell cancer suppression ability of the PNs was much higher than that of Taxol®, and likely derived from passively targeting tumor cells by the EPR effect caused to nanoparticle properties. The formulation of Taxol® is non-targeted solution which composed with Cremophor EL® (polyoxyethylated castor oil) and ethanol. So it is not able to passively targeted tumor cells. The HPNs inhibited tumor growth more efficiently than the PNs because of the presence of HA on the nanocarriers' surface, which may have targeted the tumors directly via specific binding to CD44.

Our findings suggest that the PTX nanoemulsion coated with HA actively targets CD44. PNs without HA only slightly

inhibited cancer cell growth, while HA coatings enhanced the efficacy of the treatment. Body weight loss in mice treated with Taxol[®] was greater than in mice treated with saline, PNs, or HPNs ($p > 0.05$). This may imply that Taxol[®] exerts greater toxicity and causes serious adverse effects. Mice treated with PNs and HPNs displayed a less than 10% change in body weight ($p < 0.05$). This may indicate that PNs and HPNs exert low toxicity and cause few side effects (Liu *et al.*, 2015). No significant changes in organ weight were observed, although it is unknown whether this correlates with low to no toxicity. We conclude that HPN is a highly effective nanocarrier for actively delivering PTX to non-small cell lung carcinomas over-expressing CD44s. In the future, we would like to investigate the *in vivo* antitumor efficacy studies of nude mice treated with saline, Taxol[®], PNs, or HPNs in a CD44-overexpressing breast cancer cell xenograft tumor.

REFERENCES

- Baek, J. S., Shin, S. C. and Cho, C. W. (2012) Effect of lipid on physicochemical properties of solid lipid nanoparticle of paclitaxel. *Int. J. Pharm. Investig.* **42**, 279-283.
- Battistini, F. D., Flores-Martin, J., Olivera, M. E., Genti-Raimondi, S. and Manzo, R. H. (2014) Hyaluronan as drug carrier. The *in vitro* efficacy and selectivity of Hyaluronan-Doxorubicin complexes to affect the viability of overexpressing CD44 receptor cells. *Eur. J. Pharm. Sci.* **65**, 122-129.
- Danhier, F., Vroman, B., Lecouturier, N., Crockart, N., Pourcelle, V., Freichels, H., Jérôme, C., Marchand-Brynaert, J., Feron, O. and Préat, V. (2009) Targeting of tumor endothelium by RGD-grafted PLGA-nanoparticles loaded with paclitaxel. *J. Control. Release* **140**, 166-173.
- Davis, M. E., Chen, Z. G. and Shin, D. M. (2008) Nanoparticle therapeutics: an emerging treatment modality for cancer. *Nat. Rev. Drug Discov.* **7**, 771-782.
- Fang, J., Nakamura, H. and Maeda, H. (2011) The EPR effect: Unique features of tumor blood vessels for drug delivery, factors involved, and limitations and augmentation of the effect. *Adv. Drug Deliv. Rev.* **63**, 136-151.
- Journo-Gershefeld, G., Kapp, D., Shamay, Y., Kopeček, J. and David, A. (2012) Hyaluronan oligomers-HPMA copolymer conjugates for targeting paclitaxel to CD44-overexpressing ovarian carcinoma. *Pharm. Res.* **29**, 1121-1133.
- Kim, J. E. and Park, Y. J. (2016) High paclitaxel-loaded and tumor cell-targeting hyaluronan-coated nanoemulsions. *Colloids Surf. B Biointerfaces*. [Epub ahead of print].
- Kirtane, A. R., Narayan, P., Liu, G. and Panyam, J. (2016) Polymer-surfactant nanoparticles for improving oral bioavailability of doxorubicin. *Int. J. Pharm. Investig.* [Epub ahead of print].
- Liebmann, J., Cook, J. A. and Mitchell, J. B. (1993) Cremophor EL, solvent for paclitaxel, and toxicity. *Lancet* **342**, 1428.
- Liu, D., Liu, F., Liu, Z., Wang, L. and Zhang, N. (2011a) Tumor specific delivery therapy by double-targeted nanostructured lipid carriers with anti-VEGFR-2 antibody. *Mol. Pharm.* **8**, 2291-2301.
- Liu, D., Liu, Z., Wang, L., Zhang, C. and Zhang, N. (2011b) Nanostructured lipid carriers as novel carrier for parenteral delivery of docetaxel. *Colloids Surf. B Biointerfaces* **85**, 262-269.
- Liu, P., Situ, J. Q., Li, W. S., Shan, C. L., You, J., Yuan, H., Hu, F. Q. and Du, Y. Z. (2015) High tolerated paclitaxel nano-formulation delivered by poly (lactic-co-glycolic acid)-g-dextran micelles to efficient cancer therapy. *Nanomedicine* **11**, 855-866.
- Matsubara, Y., Katoh, S., Taniguchi, H., Oka, M., Kadota, J. and Kohno, S. (2000) Expression of CD44 variants in lung cancer and its relationship to hyaluronan binding. *J. Int. Med. Res.* **28**, 78-90.
- Mercê, A. L., Marques Carrera, L. C., Santos Romanholi, L. K. and Lobo Recio, M. A. (2002) Aqueous and solid complexes of iron (III) with hyaluronic acid: potentiometric titrations and infrared spectroscopy studies. *J. Inorg. Biochem.* **89**, 212-218.
- Mizrahy, S., Raz, S. R., Hasgaard, M., Liu, H., Soffer-Tsur, N., Cohen, K., Dvash, R., Landsman-Milo, D., Bremer, M. G., Moghimi, S. M. and Peer, D. (2011) Hyaluronan-coated nanoparticles: the influence of the molecular weight on CD44-hyaluronan interactions and on the immune response. *J. Control. Release* **156**, 231-238.
- Orr, G. A., Verdier-Pinard, P., McDaid, H. and Horwitz, S. B. (2003) Mechanisms of Taxol resistance related to microtubules. *Oncogene* **22**, 7280-7295.
- Othman, T., Goto, S., Lee, J. B., Taimura, A., Matsumoto, T. and Kosaka, M. (2001) Hyperthermic enhancement of the apoptotic and antiproliferative activities of paclitaxel. *Pharmacology* **62**, 208-212.
- Park, J. H., Cho, H. J., Yoon, H. Y., Yoon, I. S., Ko, S. H., Shim, J. S., Cho, J. H., Park, J. H., Kim, K., Kwon, I. C. and Kim, D. D. (2014) Hyaluronic acid derivative-coated nanohybrid liposomes for cancer imaging and drug delivery. *J. Control. Release* **174**, 98-108.
- Sim, T., Lim, C., Hoang, N. H., Joo, H., Lee, J. W., Kim, D.-w., Lee, E. S., Youn, Y. S., Kim, J. O. and Oh, K. T. (2016) Nanomedicines for oral administration based on diverse nanoplatform. *Int. J. Pharm. Investig.* **46**, 351-362.
- Singla, A. K., Garg, A. and Aggarwal, D. (2002) Paclitaxel and its formulations. *Int. J. Pharm.* **235**, 179-192.
- Xin, D., Wang, Y. and Xiang, J. (2010) The use of amino acid linkers in the conjugation of paclitaxel with hyaluronic acid as drug delivery system: synthesis, self-assembled property, drug release, and *in vitro* efficiency. *Pharm. Res.* **27**, 380-389.
- Xiong, Y., Zhao, Y., Miao, L., Lin, C. M. and Huang, L. (2016) Co-delivery of polymeric metformin and cisplatin by self-assembled core-membrane nanoparticles to treat non-small cell lung cancer. *J. Control. Release* **244**, 63-73.
- Yang, X. Y., Li, Y. X., Li, M., Zhang, L., Feng, L. X. and Zhang, N. (2013) Hyaluronic acid-coated nanostructured lipid carriers for targeting paclitaxel to cancer. *Cancer Lett.* **334**, 338-345.
- Zhan, C., Gu, B., Xie, C., Li, J., Liu, Y. and Lu, W. (2010) Cyclic RGD conjugated poly (ethylene glycol)-co-poly (lactic acid) micelle enhances paclitaxel anti-glioblastoma effect. *J. Control. Release* **143**, 136-142.
- Zhao, D., Gong, T., Fu, Y., Nie, Y., He, L. L., Liu, J. and Zhang, Z. R. (2008) Lyophilized Cheliensis A submicron emulsion for intravenous injection: characterization, *in vitro* and *in vivo* antitumor effect. *Int. J. Pharm.* **357**, 139-147.
- Zhao, P., Wang, H., Yu, M., Cao, S., Zhang, F., Chang, J. and Niu, R. (2010) Paclitaxel-loaded, folic-acid-targeted and TAT-peptide-conjugated polymeric liposomes: *in vitro* and *in vivo* evaluation. *Pharm. Res.* **27**, 1914-1926.
- Zhao, P., Wang, H., Yu, M., Liao, Z., Wang, X., Zhang, F., Ji, W., Wu, B., Han, J., Zhang, H., Wang, H., Chang, J. and Niu, R. (2012) Paclitaxel loaded folic acid targeted nanoparticles of mixed lipid-shell and polymer-core: *in vitro* and *in vivo* evaluation. *Eur. J. Pharm. Biopharm.* **81**, 248-256.